Journal of Geodesy (2000) 74: 552–560

Journal of Geodesy

The gravitational potential and its derivatives for the prism

D. Nagy (✉)[1], G. Papp[2], J. Benedek[2]

[1] Geodetic Survey Division, Geomatics Canada, 615 Booth Street, Ottawa, Canada K1A 0E9, e-mail: nagy@nrcan.gc.ca
[2] Geodetic and Geophysical Research Institute of the Hungarian Academy of Sciences, POB 5, H-9401 Sopron, Hungary

Received: 18 August 1999 / Accepted: 15 June 2000

Abstract. As a simple building block, the right rectangular parallelepiped (prism) has an important role mostly in local gravity field modelling studies when the so called flat-Earth approximation is sufficient. Its primary (methodological) advantage follows from the simplicity of the rigorous and consistent analytical forms describing the different gravitation-related quantities. The analytical forms provide numerical values for these quantities which satisfy the functional connections existing between these quantities at the level of numerical precision applied. Closed expressions for the gravitational potential of the prism and its derivatives (up to the third order) are listed for easy reference.

Key words: Rectangular parallelepiped – Prism – Gravitational potential – Derivatives

1 Introduction

Because of its simplicity, the right rectangular parallelepiped (prism) and its various potential-related closed expressions have been the focus of interest for nearly two centuries. Using prisms, any three-dimensional (3D) density distribution can be approximated with any desired accuracy. Naturally, the density can be assigned to each prism independently of any neighbouring densities.

Although the rectangular geometry of the prism, which implies flat-Earth approximation, limits its applicability over extended areas, it is still a good alternative for the description of the density distribution and especially useful in model studies. The use of spherical models requires extensive computational efforts because of the spherical harmonic expansion of Newton's gravitational potential. The necessary truncation of the series expansion provides a resolution lower than that which can usually be obtained from the spatial resolution of the density distribution (see e.g. Papp and Wang 1996). Therefore, the spherical model may not be as advantageous for very detailed local modelling. For instance, in order to resolve 1×1 km density information in spherical geometry, a spherical harmonics expansion up to degree and order 36 000 would be necessary.

Some of the earliest investigations date back to replies to a problem posed to determine the gravitational attraction of two specially placed prisms (Zach 1811).

The first answer for the vertical component of the gravitational attraction for the prism was provided by Mollweide (1813). Independently, Bessel (1813) gave the closed expression of the potential (the term was not coined at that time) for the prism. Later, in connection with arc measurement in India, a general expression for the attraction of a prism on the three components of the deflection of the vertical was derived (Everest 1830).

Almost a century later, a number of corrections to the measured data had to be carried out for the interpretation of the results of Eötvös torsion balance measurements. In order to model some of these corrections, it became necessary to develop the required mathematical expressions. Thus, for example, the second derivatives needed in these computations were obtained for the prism by Lancaster-Jones (1928). Mader (1951) and Haáz (1953) provided summaries of most of the equations related to the prism.

Later, the vertical component of the potential was derived by Nagy (1966a) in connection with gravity field modelling studies. He also gave the expressions to calculate geoidal height, gravity anomaly[1], and the components of the deflections of the vertical (Nagy 1980).

Today's computational power can easily handle the complex expressions, even for very large 3D models. Because of this, and also to provide easy access to the required expressions, it seems reasonable to list the closed expressions in a unified fashion to aid different modelling requirements. To our knowledge, such a summary in English is not readily available. Thus, our

[1] There is a misprint in Nagy (1966a): in Eq. (5), y should be replaced by z.

aim here is to present as complete and unified a collection as possible of the relations, up to the third derivative, of the potential for the prism.

2 The equations

To date, most of the applications of volume element modelling have been aimed at the reproduction of gravity anomalies or other gravity field related quantities observed *on* and *above* the surface of the Earth, that is, outside of the masses generating the investigated anomaly. This condition was implicitly implied in the derivation of the equations resulting in a loss of generality which, in some cases, can be a disadvantage. That is why the validity of the equations in the whole 3D space R^3 is also investigated in the following and is extended up to the third partial derivatives of the gravitational potential. The study and interpretation of the fine structure of the gravitational field of the Earth require these quantities, which can be obtained by forward-modelling computations.

Before listing the expressions, a few simplifications will be introduced in order to reduce the complexity of the form of the equations. There is no standard approach or notation followed by the authors involved in the various phases of the development of this subject area. Therefore, in some cases, it may not be obvious that the expressions derived differently are identical if they are evaluated on the same domain of R^3, that is, outside or inside of the prism. Approaching the corners, edges or surface planes of the prism the different forms behave differently because of the different analytical forms of the functions used in deriving these expressions. Some of the functions at the limits are defined by simple substitution, whereas others require obtaining the limits for their indeterminate value. These functions, however, should take on the same value whether obtained from direct substitution or by applying the limiting process.

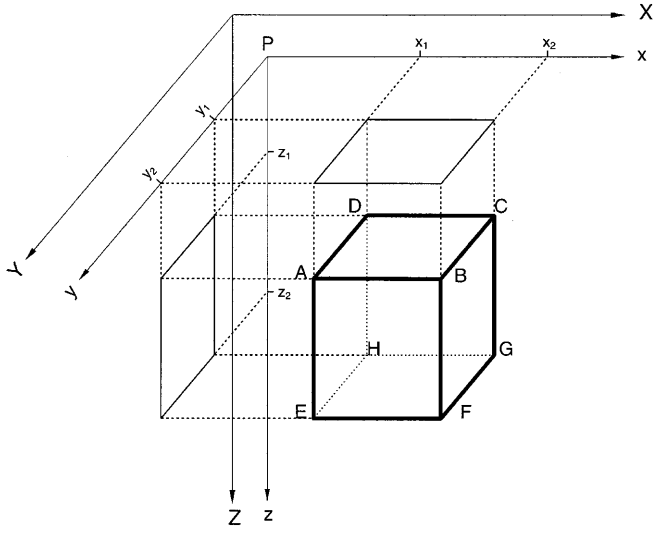

Fig. 1. Notation used for the definition of a prism

The notations used in this paper are shown in Fig. 1. The prism is bounded by planes parallel to the coordinate planes and defined by the coordinates X_1, X_2, Y_1, Y_2, Z_1 and Z_2, respectively in a left-handed coordinate system, whereas the computation point P is located at X, Y and Z.

The first simplification is to define the computation point $P(X, Y, Z)$ as the origin of the coordinate system of the computations. Practically, this means that the coordinates defining the prism have to be transformed by a simple 3D shift if the orientation of the coordinate system is not changed. This gives the following:

$$\begin{aligned} x_1 &= X_1 - X_P \\ x_2 &= X_2 - X_P \\ y_1 &= Y_1 - Y_P \\ y_2 &= Y_2 - Y_P \\ z_1 &= Z_1 - Z_P \\ z_2 &= Z_2 - Z_P \end{aligned} \tag{1}$$

This simplification can be done without any loss of generality. Thus all computed values are valid at $O(0,0,0) \equiv P(X, Y, Z)$, i.e. at $x = 0$, $y = 0$ and $z = 0$.

Next, two closely related functions will be defined:

$$u(P) = \int_v \frac{\mathrm{d}x\,\mathrm{d}y\,\mathrm{d}z}{r} = \int_{x_1}^{x_2}\int_{y_1}^{y_2}\int_{z_1}^{z_2} \frac{\mathrm{d}x\,\mathrm{d}y\,\mathrm{d}z}{r} \tag{2}$$

where

$$r(x,y,z) = \sqrt{x^2 + y^2 + z^2}$$

and

$$U(P) = u(P)G\rho \tag{3}$$

In the above, $U(P)$ is the gravitational potential at P point obtained by carrying out the volume (triple) integration over the body v in question (in this case, this will be the prism *ABCDEFGH*; see Fig. 1), with a constant density ρ. Here G is the gravitational constant. Since ρ is constant, u and its first derivatives – similarly to the potential U – exist and are continuous in the whole R^3 (Tychonov and Samarski 1964, pp. 357–370). The partial derivatives of u higher than order one are defined and continuous at every point in the vicinity of which ρ and its partial derivatives are continuous (Tychonov and Samarski 1964). In practice, this means that there is no density discontinuity at point P.

The result of the integration of Eq. (2) over v can be given in the following form:

$$\begin{aligned} u(P) = \Bigg|\Bigg|\Bigg| & xy\ln(z+r) + yz\ln(x+r) + zx\ln(y+r) \\ & - \frac{x^2}{2}\tan^{-1}\frac{yz}{xr} - \frac{y^2}{2}\tan^{-1}\frac{zx}{yr} - \frac{z^2}{2}\tan^{-1}\frac{xy}{zr}\Bigg|_{x_1}^{x_2}\Bigg|_{y_1}^{y_2}\Bigg|_{z_1}^{z_2} \end{aligned} \tag{4}$$

Substituting all the limits results in 48 terms.

As the derivations of these expressions are not the subject of this discussion, the interested reader may consult, for example, Bessel (1813, p. 84), Macmillan (1930, pp. 78–79), Mader (1951, p. 6) and Haáz (1953, p. 64) for details. Although the potential U exists and is continuous in R^3, Eq. (4) as an *analytical solution* of Eq. (2) is *not* defined in every point of R^3, which may cause problems in direct numerical evaluation. At those points where any of the terms on the right-hand side of Eq. (4) are not defined, the specific term should be set to zero because it has a finite (zero) limit. For example, the first term on the right-hand side of Eq. (4) is not defined if one of the corners of the prism coincides with the origin of the computation (P) because only a limit exists for the values (e.g. $x_1 = y_1 = z_1 = 0$), defining the computation point to be substituted:

$$\lim_{(x,y,z)\to(0,0,0)} xy\ln(z+r) = 0 \tag{5}$$

Similarly, it can be shown that all other terms showing such indeterminate characteristics have zero limit at the points located at corners, edges and planes of the prism. In this way the continuity of Eq. (4) can be extended to R^3. As an example, for a point P situated on one of the edges of the prism ($\overline{AD} : x_1 \neq 0, x_2 \neq 0,\ y_1 = z_1 = 0$), the limit of u is

$$\begin{aligned} u(P) = \lim_{(\varepsilon_1,\varepsilon_2,\varepsilon_3)\to(0,0,0)} \Bigg|\Bigg|\Bigg| & xy\ln(z+r) + yz\ln(x+r) \\ & + zx\ln(y+r) - \frac{x^2}{2}\tan^{-1}\frac{yz}{xr} - \frac{y^2}{2}\tan^{-1}\frac{zx}{yr} \\ & - \frac{z^2}{2}\tan^{-1}\frac{xy}{zr}\Bigg|_{x_1+\varepsilon_1}^{x_2+\varepsilon_1}\Bigg|_{\varepsilon_2}^{y_2+\varepsilon_2}\Bigg|_{\varepsilon_3}^{z_2+\varepsilon_3} \end{aligned} \tag{6}$$

where $\varepsilon_1, \varepsilon_2$ and ε_3 are arbitrarily small quantities which never have zero value at the same time ($\varepsilon_1^2 + \varepsilon_2^2 + \varepsilon_3^2 \neq 0$). The first four terms on the right-hand side of Eq. (6) are defined at the computation point (P) and their limits are equal to the values obtained by simple substitution. The limits of the last two terms are given by

$$\begin{aligned} & \lim_{(\varepsilon_1,\varepsilon_2,\varepsilon_3)\to(0,0,0)} \Bigg|\Bigg|\Bigg| -\frac{y^2}{2}\tan^{-1}\frac{zx}{yr} - \frac{z^2}{2}\tan^{-1}\frac{xy}{zr}\Bigg|_{x_1+\varepsilon_1}^{x_2+\varepsilon_1}\Bigg|_{\varepsilon_2}^{y_2+\varepsilon_2}\Bigg|_{\varepsilon_3}^{z_2+\varepsilon_3} \\ & = -\frac{y_2^2}{2}\tan^{-1}\frac{z_2x_2}{y_2r(x_2,y_2,z_2)} - \frac{z_2^2}{2}\tan^{-1}\frac{x_2y_2}{z_2r(x_2,y_2,z_2)} \\ & \quad + \frac{y_2^2}{2}\tan^{-1}\frac{z_2x_1}{y_2r(x_1,y_2,z_2)} + \frac{z_2^2}{2}\tan^{-1}\frac{x_1y_2}{z_2r(x_1,y_2,z_2)} \end{aligned} \tag{7}$$

That is, Eq. (7) results in four terms, because the other 12 terms are equal to zero at the limit, irrespective of the direction of approach. Other situations concerning the location of P can be discussed in a similar way and thus it can be shown that u given by Eq. (4) can be extended in R^3 continuously.

The gradient $(\partial u/\partial x, \partial u/\partial y, \partial u/\partial z)$ of u is also continuous in R^3. Therefore, for example, the vertical component of u can be obtained by differentiating Eq. (4) with respect to z, which gives

$$u_z(P) = \Bigg|\Bigg|\Bigg| x\ln(y+r) + y\ln(x+r) - z\tan^{-1}\frac{xy}{zr}\Bigg|_{x_1}^{x_2}\Bigg|_{y_1}^{y_2}\Bigg|_{z_1}^{z_2} \tag{8}$$

The same form is obtained if the kernel function of Eq. (2) is partially differentiated before the integration

$$\frac{\partial u}{\partial z} = \int_v \frac{\partial}{\partial z}\frac{\mathrm{d}x\,\mathrm{d}y\,\mathrm{d}z}{r} \tag{9}$$

Carrying out the partial differentiation gives

$$\frac{\partial u}{\partial z} \equiv u_z = -\int_v \frac{z\,\mathrm{d}x\,\mathrm{d}y\,\mathrm{d}z}{r^3} \tag{10}$$

The remaining two derivatives, u_x and u_y, can be obtained from u_z by cyclic permutation

$$u_x(P) = \Bigg|\Bigg|\Bigg| y\ln(x+r) + z\ln(y+r) - x\tan^{-1}\frac{yz}{xr}\Bigg|_{x_1}^{x_2}\Bigg|_{y_1}^{y_2}\Bigg|_{z_1}^{z_2} \tag{11}$$

$$u_y(P) = \Bigg|\Bigg|\Bigg| z\ln(y+r) + x\ln(x+r) - y\tan^{-1}\frac{zx}{yr}\Bigg|_{x_1}^{x_2}\Bigg|_{y_1}^{y_2}\Bigg|_{z_1}^{z_2} \tag{12}$$

Evaluating Eqs. (8), (11) and (12), the same problem of indetermination arises as when Eq. (4) is considered. For example, although U_z definitely exists on the *interior* of the planes [Int($ABCD \cup EFGH$)] representing a density discontinuity and bounding the prism which are parallel to the XY coordinate plane (Fig. 2) (Tychonov and Samarski 1964, pp. 357–370), u_z is *not* defined there. However, zero limits for the critical terms in Eqs. (11), (12) and (8) at these locations do exist (Fig. 2). Therefore at those points where any of the terms of the right-hand side of Eqs. (8), (11) and (12) are not defined, the specific term should be set to zero in practical computations. Consequently u_x, u_y and u_z can be extended in R^3 continuously. If P is a point (e.g. a corner of the prism at D: $x_1 = y_1 = z_1 = 0$; Fig. 1) where, for example, u_z is not defined, we obtain

$$\begin{aligned} u_z(P) = \lim_{(\varepsilon_1,\varepsilon_2,\varepsilon_3)\to(0,0,0)} \Bigg|\Bigg|\Bigg| & x\ln(y+r) + y\ln(x+r) \\ & - z\tan^{-1}\frac{xy}{zr}\Bigg|_{\varepsilon_1}^{x_2+\varepsilon_1}\Bigg|_{\varepsilon_2}^{y_2+\varepsilon_2}\Bigg|_{\varepsilon_3}^{x_2+\varepsilon_3} \\ = {} & x_2\ln(y_2 + r(x_2,y_2,z_2)) - x_2\ln(y_2 + r(x_2,y_2,0)) \\ & - x_2\ln(r(x_2,0,z_2)) + x_2\ln(r(x_2,0,0)) \\ & + y_2\ln(x_2 + r(x_2,y_2,z_2)) - y_2\ln(x_2 + r(x_2,y_2,0)) \\ & - y_2\ln(r(0,y_2,z_2)) + y_2\ln(r(0,y_2,0)) \\ & - z_2\tan^{-1}\frac{x_2y_2}{z_2r(x_2,y_2,z_2)} \end{aligned} \tag{13}$$

Theoretically, Eq. (13) should contain 24 terms. However, nine of them have zero limit at the corresponding

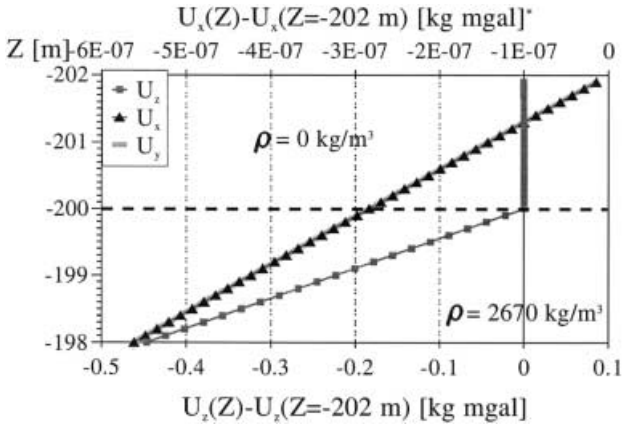

Fig. 2. Behaviour of the first derivatives of U near a density interface represented by the upper bounding plane $ABCD$ of a prism having a constant density of 2670 kg/m^3 ($z_1 = -200$ m). The values are computed along a straight line displayed on the chart. * The same axis is used for U_y

integration limits whose value can also be obtained by simple substitution. Six of them have limits

$$\lim_{(x,y,z)\to(0,0,0)} x\ln(y+r(x,y,z)) = \lim_{(x,y,z)\to(0,0,0)} y\ln(x+r(x,y,z)) = 0$$

$$\lim_{(x,y,z\neq 0)\to(0,0,0)} z\tan^{-1}\frac{xy}{zr} = 0$$

The components of the gradient of the gravitational potential can easily be obtained as the product of the quantities given by Eqs. (8), (11) and (12) and $G\rho$.

Generally, the second derivatives of function u are not defined on the boundary surface of the prism if it represents an interface of density discontinuity. This indeterminate character of the derivatives depends on which derivatives is considered on which plane of the bounding surface. The possible combinations are listed in Table 1. However, four examples of the indeterminate character are given.

2.1 Example 1

The computation point P is an inner point of the surface plane [Int($ABCD$); Fig. 1] of the prism which coincides with the xy coordinate plane. The limit is given as

$$\begin{aligned}
&\lim_{P'\to P} u_{zz}(P') \\
&= \lim_{(\varepsilon_1,\varepsilon_2,\varepsilon_3\neq 0)\to(0,0,0)} \left|\left|\left| -\tan^{-1}\frac{xy}{zr}\right|_{x_1+\varepsilon_1}^{x_2+\varepsilon_1}\right|_{y_1+\varepsilon_2}^{y_2+\varepsilon_2}\right|_{\varepsilon_3}^{z_2+\varepsilon_3} \\
&= \operatorname{sign}(\varepsilon_3)2\pi - \tan^{-1}\frac{x_2y_2}{z_2r(x_2,y_2,z_2)} \\
&\quad + \tan^{-1}\frac{x_1y_2}{z_2r(x_1,y_2,z_2)} - \tan^{-1}\frac{x_1y_1}{z_2r(x_1,y_1,z_2)} \\
&\quad + \tan^{-1}\frac{x_2y_1}{z_2r(x_2,y_1,z_2)} \qquad (14)
\end{aligned}$$

where $(\varepsilon_1, \varepsilon_2, \varepsilon_3 \neq 0) \to (0,0,0)$ means that $P' \notin xy$. The sign function in Eq. (14) indicates that the limit of u_{zz} at P depends on which half-space the point P is being approached from. The difference between the two limits belonging to the half-spaces is always 4π according to the Poisson equation

$$\Delta U = G\rho\Delta u = -4\pi G\rho$$

where $\Delta u = u_{xx} + u_{yy} + u_{zz}$ is the divergence of the function u. The derivatives u_{xx} and u_{yy} behave similarly to u_{zz} on the surface planes Int($ABFE \cup DCGH$) and Int ($ADHE \cup BCGH$), respectively.

Figure 3 shows how the homogeneous second derivatives of U change inside two joining prisms of different density ($\rho_1 = 2400\,\text{kg/m}^3$, $\rho_2 = 2670\,\text{kg/m}^3$ if the computation point P is moved along a straight line perpendicular to the interface of density discontinuity. The Poisson equation makes it possible to reconstruct the density of the prisms from the summation of the

Table 1. List of all cases regarding the location of the computation point P

Function	Domain								
	1	2	3	4	5	6	7	8	9
u, u_x, u_y, u_z	∃	∃	∃	∃	∃	∃	∃	∃	∃
u_{xx}	∃	∃	∃	∃	∄[a]	∄[b]	∃	∄[b]	∄[c]
u_{xy}	∃	∃	∃	∃	∃	∃	∃	∄[d]	∄[c]
u_{xz}	∃	∃	∃	∃	∃	∄[d]	∃	∃	∄[c]
u_{yy}	∃	∃	∃	∄[a]	∃	∃	∄[b]	∄[b]	∄[c]
u_{yz}	∃	∃	∃	∃	∃	∃	∄[d]	∃	∄[c]
u_{zz}	∃	∃	∄[a]	∃	∃	∄[b]	∄[b]	∃	∄[c]
Third-order partial derivatives	∃	∃	∄	∄∄	∄	∄	∄	∄	

[a] See example 1
[b] See example 2
[c] See example 3
[d] See example 4
Domain 1 ≡ Ext($ABCDEFGH$)
Domain 2 ≡ Int($ABCDEFGH$)
Domain 3 ≡ Int($ABCD \cup EFGH$)
Domain 4 ≡ Int($ADHE \cup BCGF$)
Domain 5 ≡ Int($ABFE \cup DCGH$)
Domain 6 ≡ Int($\overline{AB} \cup \overline{DC} \cup \overline{HG} \cup \overline{EF}$)
Domain 7 ≡ Int($\overline{AD} \cup \overline{BC} \cup \overline{FG} \cup \overline{EH}$)
Domain 8 ≡ Int($\overline{AE} \cup \overline{BF} \cup \overline{CG} \cup \overline{DH}$)
Domain 9 ≡ {A, B, C, D, E, F, G, H}
∃ – exists: the given formulae can be used; ∄ – does not exist: the given formulae cannot be used; Int – interior of the domain; Ext – exterior of the domain

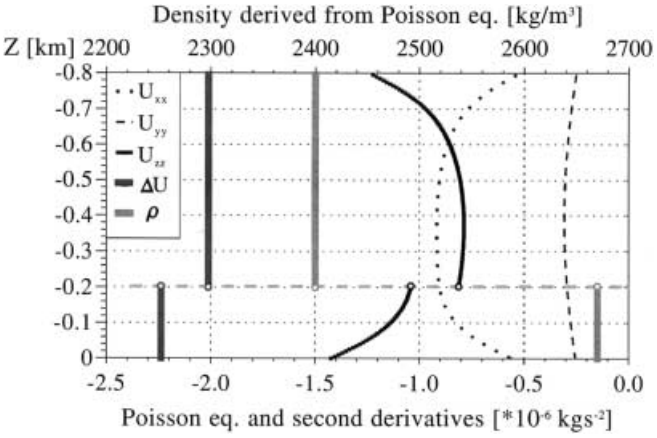

Fig. 3. Numerical check of the validity of Poisson equation ($\Delta U = -4\pi G\rho$) inside two joining prisms having different density. The second derivatives (U_{xx}, U_{yy}, U_{zz}) were computed from Eqs. (22), (23) and (24), respectively, by using the factor $G\rho$. The density values were obtained by using Eq. (15). *Horizontal dashed line* at $z = -0.2$ km represents the density interface

calculated second derivatives (U_{xx}, U_{yy}, U_{zz}) and in this way the performance of the formulae can be checked numerically

$$\rho(P) = \Delta U(P)/-4\pi G \tag{15}$$

2.2 Example 2

The computation point P is situated on the edge $\overline{CD}$ of the prism coinciding with the y axis (Fig. 1)

$$\begin{aligned}
&\lim_{P'\to P} u_{zz}(P') \\
&= \lim_{(\varepsilon_1,\varepsilon_2,\varepsilon_3\neq 0)\to(0,0,0)} \left|\left|\left| -\tan^{-1}\frac{xy}{zr}\right|_{\varepsilon_1}^{x_2+\varepsilon_1}\right|_{y_1+\varepsilon_2}^{y_2+\varepsilon_2}\right|_{\varepsilon_3}^{z_2+\varepsilon_3} \\
&= \operatorname{sign}(\varepsilon_3)\pi - \tan^{-1}\frac{x_2y_2}{z_2r(x_2,y_2,z_2)} \\
&\quad + \tan^{-1}\frac{x_2y_1}{z_2r(x_2,y_1,z_2)} + \lim_{k\to 0}\tan^{-1}\frac{k\alpha y_1}{k\beta r(0,y_1,0)} \\
&\quad - \lim_{k\to 0}\tan^{-1}\frac{k\alpha y_2}{k\beta r(0,y_2,0)}
\end{aligned} \tag{16}$$

where $\varepsilon_1 = k\alpha$ and $\varepsilon_3 = k\beta$. Equation (16) shows that the limit of y_{zz} does not exist because its last two terms give different values if α and β, which determine the direction of approach, are selected arbitrarily.

2.3 Example 3

The computation point P is located on the corner D of the prism (Fig. 1)

$$\begin{aligned}
&\lim_{P'\to P} u_{zz}(P') \\
&= \lim_{(\varepsilon_1,\varepsilon_2,\varepsilon_3\neq 0)\to(0,0,0)} \left|\left|\left| -\tan^{-1}\frac{xy}{zr}\right|_{\varepsilon_1}^{x_2+\varepsilon_1}\right|_{\varepsilon_2}^{y_2+\varepsilon_2}\right|_{\varepsilon_3}^{z_2+\varepsilon_3} \\
&= \operatorname{sign}(\varepsilon_3)\frac{\pi}{2} - \tan^{-1}\frac{x_2y_2}{z_2r(x_2,y_2,z_2)} \\
&\quad - \lim_{k\to 0}\tan^{-1}\frac{k\alpha y_2}{k\beta r(0,y_2,0)} + \lim_{k\to 0}\tan^{-1}\frac{k\alpha k\gamma}{k\beta r(k\alpha,k\gamma,k\beta)} \\
&\quad - \lim_{k\to 0}\tan^{-1}\frac{x_2k\gamma}{k\beta r(x_2,0,0)}
\end{aligned} \tag{17}$$

where $\varepsilon_2 = k\gamma$ and γ determines the direction of approach. For the same reason as in Example 2, u_{zz} has no limit at P.

2.4 Example 4

The computation point is on the line $\overline{AE}$

$$\begin{aligned}
&\lim_{P'\to P} u_{xy}(P') \\
&= \lim_{(\varepsilon_1,\varepsilon_2,\varepsilon_3)\to(0,0,0);\varepsilon_1^2+\varepsilon_2^2\neq 0} \left|\left|\left| \ln(z+r)\right|_{\varepsilon_1}^{x_2+\varepsilon_1}\right|_{\varepsilon_2}^{y_2+\varepsilon_2}\right|_{z_1+\varepsilon_3}^{z_2+\varepsilon_3} \\
&= \ln(z_2 + r(x_2,y_2,z_2)) - \ln(z_1 + r(x_2,y_2,z_1)) \\
&\quad - \ln(z_2 + r(x_2,0,z_2)) + \ln(z_1 + r(x_2,0,z_1)) \\
&\quad - \ln(z_2 + r(0,y_2,z_2)) + \ln(z_1 + r(0,y_2,z_1)) + \ln(2z_2) \\
&\quad - \lim_{\substack{(\varepsilon_1,\varepsilon_2,\varepsilon_3)\to(0,0,0) \\ \varepsilon_1^2+\varepsilon_2^2\neq 0}} \ln(z_1 + \varepsilon_3 + r(\varepsilon_1,\varepsilon_2,z_1+\varepsilon_3)) = \infty
\end{aligned} \tag{18}$$

where $z_1 < 0$ whereas $z_2 > 0$. Equation (18) shows that all the edges which are parallel to the z axis consist of singular points for u_{xy}.

In cases where the second derivatives exist, the following expressions can be used:

$$u_{xz}(P) = \left|\left|\ln(y+r)\right|_{x_1}^{x_2}\right|_{y_1}^{y_2}\Big|_{z_1}^{z_2} \tag{19}$$

$$u_{yz}(P) = \left|\left|\ln(x+r)\right|_{x_1}^{x_2}\right|_{y_1}^{y_2}\Big|_{z_1}^{z_2} \tag{20}$$

$$u_{xy}(P) = \left|\left|\ln(z+r)\right|_{x_1}^{x_2}\right|_{y_1}^{y_2}\Big|_{z_1}^{z_2} \tag{21}$$

$$u_{xx}(P) = \left|\left|\left| -\tan^{-1}\frac{yz}{xr}\right|_{x_1}^{x_2}\right|_{y_1}^{y_2}\right|_{z_1}^{z_2} \tag{22}$$

$$u_{yy}(P) = \left|\left|\left| -\tan^{-1}\frac{zx}{yr}\right|_{x_1}^{x_2}\right|_{y_1}^{y_2}\right|_{z_1}^{z_2} \tag{23}$$

$$u_{zz}(P) = \left|\left|\left| -\tan^{-1}\frac{xy}{zr}\right|_{x_1}^{x_2}\right|_{y_1}^{y_2}\right|_{z_1}^{z_2} \tag{24}$$

The indeterminate characteristics of the second derivatives of u are inherited by the third derivatives. If P is an inner point of a surface plane of the prism, then limits for the third derivatives exists. On the edges and corners of the prism, the limits are non-existent. Where the third derivatives do exist, the following expressions can be used:

$$u_{x\,x\,x}(P) = \left|\left|\left| \frac{yz}{r}\left(\frac{1}{x^2+z^2}+\frac{1}{x^2+y^2}\right)\right|_{x_1}^{x_2}\right|_{y_1}^{y_2}\right|_{z_1}^{z_2} \tag{25}$$

$$u_{y\,y\,y}(P) = \left|\left|\left| \frac{xz}{r}\left(\frac{1}{y^2+z^2}+\frac{1}{y^2+x^2}\right)\right|_{x_1}^{x_2}\right|_{y_1}^{y_2}\right|_{z_1}^{z_2} \tag{26}$$

$$u_{z\,z\,z}(P) = \left|\left|\left| \frac{xy}{r}\left(\frac{1}{x^2+z^2}+\frac{1}{y^2+z^2}\right)\right|_{x_1}^{x_2}\right|_{y_1}^{y_2}\right|_{z_1}^{z_2} \tag{27}$$

$$u_{x\,x\,y}(P) = \left|\left|\left| -\frac{zx}{r}\left(\frac{1}{x^2+y^2}\right)\right|_{x_1}^{x_2}\right|_{y_1}^{y_2}\right|_{z_1}^{z_2} \tag{28}$$

$$u_{x\,x\,z}(P) = \left|\left|\left| -\frac{yx}{r}\left(\frac{1}{x^2+z^2}\right)\right|_{x_1}^{x_2}\right|_{y_1}^{y_2}\right|_{z_1}^{z_2} \tag{29}$$

$$u_{y\,y\,x}(P) = \left|\left|\left| -\frac{yz}{r}\left(\frac{1}{x^2+y^2}\right)\right|_{x_1}^{x_2}\right|_{y_1}^{y_2}\right|_{z_1}^{z_2} \tag{30}$$

$$u_{y\,y\,z}(P) = \left|\left|\left| -\frac{xy}{r}\left(\frac{1}{z^2+y^2}\right)\right|_{x_1}^{x_2}\right|_{y_1}^{y_2}\right|_{z_1}^{z_2} \tag{31}$$

$$u_{z\,z\,x}(P) = \left|\left|\left| -\frac{yz}{r}\left(\frac{1}{x^2+z^2}\right)\right|_{x_1}^{x_2}\right|_{y_1}^{y_2}\right|_{z_1}^{z_2} \tag{32}$$

$$u_{z\,z\,y}(P) = \left|\left|\left| -\frac{xy}{r}\left(\frac{1}{y^2+z^2}\right)\right|_{x_1}^{x_2}\right|_{y_1}^{y_2}\right|_{z_1}^{z_2} \tag{33}$$

$$u_{x\,y\,z}(P) = \left|\left|\left| \frac{1}{r}\right|_{x_1}^{x_2}\right|_{y_1}^{y_2}\right|_{z_1}^{z_2} \tag{34}$$

Obviously, problems may also occur when $P \in \mathrm{Ext}(ABCDEFGH)$. For example u_{zz}, Eq. (24), is indeterminate in all the points where $z_1 = 0$ or $z_2 = 0$ all over R^3. A unique and finite limit, however, exists for u_{zz} if and only if $P \in \mathrm{Ext}(ABCDEFG)$. The value of u_{zz} is equal to the limit of u_{zz} at these specific points.

$$\begin{aligned} u_{zz}(P) &= \lim_{P' \to P} u_{zz}(P') \\ &= \lim_{(\varepsilon_1,\varepsilon_2,\varepsilon_3 \neq 0) \to (0,0,0)} \left|\left|\left| -\tan^{-1}\frac{xy}{zr}\right|_{x_1+\varepsilon_1}^{x_2+\varepsilon_1}\right|_{y_1+\varepsilon_2}^{y_2+\varepsilon_2}\right|_{\varepsilon_3}^{x_2+\varepsilon_3} \\ &= -\tan^{-1}\frac{x_2 y_2}{z_2 r(x_2,y_2,z_2)} + \tan^{-1}\frac{x_1 y_2}{z_2 r(x_1,y_2,z_2)} \\ &\quad -\tan^{-1}\frac{x_1 y_1}{z_2 r(x_1,y_1,z_2)} + \tan^{-1}\frac{x_2 y_1}{z_2 r(x_2,y_1,z_2)} \end{aligned} \tag{35}$$

There are only four terms in Eq. (35) instead of eight, since the four other terms ($\equiv \pi/2$) cancel out. This is caused by the fact that at least one pair of the integration limits has the same sign. Generally, the existence of the limits at those points in Ext(*ABCDEFGH* for the other derivatives discussed above can be proven in a similar way.

Because the potential function u and its partial derivatives higher than order one are continuous where they exist, the order of differentiation can be exchanged.

$$\frac{\partial}{\partial x}\left(\frac{\partial}{\partial z}\right) \equiv \frac{\partial}{\partial z}\left(\frac{\partial}{\partial x}\right) \tag{36}$$

Therefore, the *symmetric* derivatives are not listed here.

3 Applications

In the following, some examples will be given in which some of the equations presented above have been used, or can be used. In a number of cases, except high-precision terrain correction computations, where inclined top prisms are required, it is possible to built up a realistic model from a combination of a number of prisms of various sizes and densities which approximates a practical case. This process may even be automated if interfaces between geological units are known and defined in digital form (e.g. regular grid of elevation/depth data) in the area of investigation (see e.g. Kalmár et al. 1995). Such a model based on geological and/or seismological information can be checked against different quantities (e.g. gravity anomalies, geoid undulations, horizontal gradients of the gravity anomalies, etc.) of the observed gravity field (i.e. 3D gravity interpretation). This technique has been used to study the compaction of the Neogene–Quaternary sedimentary filling of the Pannonian Basin, Hungary and its relation to be observed anomalous gravity field (Papp and Kalmár 1995).

It is also possible to carry out computations for the better understanding of a particular phenomenon, which in practice cannot be obtained directly from measurements. Examples include the changes of the deflections of the vertical with elevation (size, orientation), and upward and downward continuation of the gravity field. To aid these computations, a model will be defined consisting of n prisms. Some of the equations useful for these various studies will briefly be presented.

The disturbing potential T generated by a model composed of n prisms can be derived by *physical filtering* if a suitable reference potential U_{ref} is provided (Papp 1996b)

$$T = -U_{\mathrm{ref}} + \sum_{i=1}^{n} U_i \tag{37}$$

The contribution to geoidal height, (N), is calculated as (Nagy 1980)

$$N = -\frac{T}{\gamma} \tag{38}$$

where γ is the normal gravity at the computation point. Based on this approach, the short-wavelength geoid undulations ($\lambda_N \leq 300\,\mathrm{km}$) were determined from a 3D model of the lithosphere of the Pannonian Basin and its orogenic surroundings. This yields the so-called lithospheric geoid solution for the area of investigation utilizing a general remove–restore scheme (Papp and Kalmár 1996). The different versions of this solution fit of global geopotential models and local gravimetric geoid solutions at ±(10–20) cm in terms of the standard deviation of the residual geoid undulations (Papp

1996a). The model presently contains about 180 000 rectangular prisms of different sizes representing the density distribution of the topographic masses, the Neogene–Quaternary sedimentary complex, the lower crust and the upper mantle.

The x and y components of the deflection of the vertical (ξ, η) are

$$\xi = -\frac{1}{\gamma} T_x \tag{39}$$

$$\eta = -\frac{1}{\gamma} T_y \tag{40}$$

The gravity anomaly due to the model is

$$\Delta g \equiv -T_z \tag{41}$$

As the terrain can be approximated by a number of prisms, a program for terrain correction can easily be implemented (Nagy 1966b). Once the program is implemented, it becomes possible to carry out complex computations, for example using the Monte Carlo method to study error propagation (Nagy 1966c). Synthetic Earth models can be used effectively to compare different computational algorithms to solve the same problem. Examples include the calculation of grid values from irregular data distribution (Nagy et al. 1999), to compare direct numerical integration with fast Fourier transform (FFT) techniques (Nagy 1988a, b; Nagy and Fury 1988, 1990), and to carry out benchmarking (Nagy et al. 1989). They can provide verification of computational procedure for a given problem. As an example, the solution to calculate the gravitational effect of a right circular cylinder (Nagy 1965) was checked with an equal volume approximation of a model consisting of 150 prisms (Nagy 1966a). This not only allowed the confirmation of the developed method, but also gave insight into how the gravitational effect varies with distance, depending upon the shape of the gravitating body (as the distance approaches infinity the gravity effects of the two bodies converge to the same value).

Model studies using some of the equations listed above can be used for benchmarking different computational techniques and theories because of the complex, yet easily programmable, and time-demanding computing requirement (Nagy et al. 1989; Nagy and Stacey 1991). One area of application is to establish some parameters needed in numerical computation. As an example, one can calculate the deflections of the vertical for a model by using numerical integration of the gravity values (computed at the points where the procedure requires it, say at the centres of the Hayford template). In this case, the singularity existing in the procedure of the numerical integration to obtain the deflections must be handled differently at the origin. One solution is to exclude the effect of the near region, which will introduce error into the computation. This error basically depends of the radius (r) of the area omitted from the computation. Therefore r could be determined, depending on the accuracy required, by comparing the result of numerical integration to the *exact* value obtained by direct computation of the components from Eqs. (39) and (40). This type of model study would help to link the required gravity data distribution with the achievable accuracy of the computed deflection values.

The proper programming of the formulae given in this paper for the potential and its derivatives makes computations possible over the whole of R^3. It means that the structure of the gravitational field generated by a density model can be investigated outside as well as inside the masses (where the source density is not zero) without the usual hypothesis of harmonicity. Based on this feature, Papp and Benedek (2000) made an effort to give numerical solutions for the determination of the plumbline which may require the knowledge of the derivatives of u up to degree 3.

Lastly, the use of some of the expressions in the study of the behaviour of the local equipotential (niveau) surface is mentioned. It is known from differential geometry (see e.g. Struik 1988) that six values, the three first-order (E, F, G) and the three second-order $(L, M, N$ or sometimes written as $e, f, g)$ fundamental quantities, which satisfy certain conditions, always define a niveau surface (Bonnet theorem). If the surface is given in the form $f(x, y, z) = \text{const}$ with the origin of the coordinate system on the surface and the $+z$ axis selected along the normal directed toward the interior of the surface, then the relations, using Gauss notation, are as follows:

$$E = 1 + p^2 = 1 \tag{42}$$

$$F = pq = 0 \tag{43}$$

$$G = 1 + q^2 = 1 \tag{44}$$

$$e = \frac{r}{m} = -\frac{u_{xx}}{u_z} \tag{45}$$

$$f = \frac{s}{m} = -\frac{u_{xy}}{u_z} \tag{46}$$

$$g = \frac{t}{m} = -\frac{u_{xx}}{u_z} \tag{47}$$

where

$$p = u_x \tag{48}$$

$$q = u_y \tag{49}$$

$$m = \sqrt{1 + p^2 + q^2} = 1 \tag{50}$$

$$r = -\frac{u_{xx}}{g} \tag{51}$$

$$s = -\frac{u_{xy}}{g} \tag{52}$$

$$t = -\frac{u_{yy}}{g} \tag{53}$$

Designating the principal curvatures in x and y by κ_1 and κ_2 respectively, then the *mean curvature* and the *Gaussian curvature* (sometimes called *total curvature*) are given by the following equations:

$$\frac{1}{2}(\kappa_1 + \kappa_2) = \frac{Eg - 2fF + eG}{2(EG - f^2)} \tag{54}$$

$$\kappa_1 \kappa_2 = \frac{eg - f^2}{EG - F^2} \tag{55}$$

Equations (54) and (55) give only the sum and the product of the principal curvatures. However, from

$$g(\kappa_1 - \kappa_2) = \sqrt{(u_{yy} - u_{xx})^2 + 4u_{xy}^2} \tag{56}$$

the difference is available. Thus, by adding and subtracting Eqs. (54) and (56) the individual principal curvatures can be obtained. It is noted here that, in practice, many of the quantities could be obtained as a result of the Eötvös torsion balance measurements.

Building up a suitable 3D density model, which describes the local variation of gravity (for example at an absolute gravimeter station), the relations listed above allow detailed study of the local equipotential surface and other related quantities.

4 Concluding remarks

This paper has presented the closed expressions of the potential and its derivatives, up to the third order for a prism, in a unified manner. The formulae have been generalized to apply to the whole of R^3. Therefore, they may be used to generate gravity field quantities inside and outside of a given density model. A number of applications where they can be used to study various aspects of local gravity fields are given. Model computations can provide information which may not be available from direct measurements (e.g. variation of the deflection of the vertical with height), and provide one with a better understanding of the complexities of local field variations.

Acknowledgements. The second and third authors appreciate the support of the Hungarian National Scientific Research Fund, Project Number T025318, and the Bolyai János Scholarship Committee of the Hungarian Academy of Sciences.

References

Bessel FW (1813) Auszug aus einem Schreiben des Herrn Prof. Bessel. Zach's Monatliche Correspondenz zur Beförderung der Erd- und Himmelskunde, XXVII: 80–85

Everest G (1830) An account of the measurement of an arc of the meridian.... The Royal Society. Printed by J.L. Cox, London, pp 93–104

Haáz IB (1953) Relation between the potential of the attraction of the mass contained in a finite rectangular prism and its first and second derivatives. Geofiz Közle II(7): 57–66 (in Hungarian)

Kalmár J, Papp G, Szabó T (1995) DTM-based surface and volume approximation. Geophysical applications. Comput Geosci 21: 245–257

Lancaster-Jones E (1928) The computation of Eötvös gravity effects. Tech Publ 75, The American Institute of Mining and Metallurgical Engineers, New York, pp 1–25

MacMillan WD (1930) The theory of the potential. Dover, New York

Mader K (1951) Das Newtonsche Raumpotential prismatischer Körper und seine Ableitungen bis zur dritten Ordnung. Sonderheft 11 der Österreichischen Zeitschrift für Vermessungswesen. Österreichischer Verein für Vermessungswesen, Wien

Mollweide KB (1813) Auflösung einiger die Anziehing von Linien Flächen und Köpern betreffenden Aufgaben unter denen auch die in der Monatl Corresp Bd XXIV. S. 522. vorgelegte sich findet. Zach's Monatliche Correspondenz zur Beförderung der Erd- und Himmelskunde, Bd XXVII: 26–38

Nagy D (1965) The evaluation of Heumann's lambda function and its application to calculate the gravitational effect of a right circular cylinder. Pure Appl Geophys 62: 5–12

Nagy D (1966a) The gravitational attraction of a right rectangular prism. Geophysics XXXI(2): 362–371

Nagy D (1966b) The prism method for terrain correction using digital computers. Pure Appl Geophys 102: 5–14

Nagy D (1966c) Application of the Monte Carlo Method to analyze the effect of observation errors in gravity reductions. Int Geodetic Conf Measuring Technique and Instrument Problems, Budapest, 14–20 April

Nagy D (1980) Gravity anomalies, deflections of the vertical and geoidal heights for a three-dimensional model. Acta Geod Geophys Mont Hung 15(1): 17–26

Nagy D (1988a) Fast Fourier Transform and modelling in geoid computation. Boll Geod Sci Affini Riv Istitut Geogr Militare XLVII(1): 33–43

Nagy D (1988b) Fast Fourier Transform in gravity interpretation. Acta Geod Geophys Mont Hung 23(1): 97–115

Nagy D, Fury R (1988) FFT – local gravimetric geoid determination. Proc Chapman Conf Progress in the Determination of the Earth's Gravity Field. September 13–16, Ft. landerdale, Florida, pp 91–95

Nagy D, Fury RJ (1990) Local geoid computation from gravity using the fast Fourier transform technique. Bull Geod 64: 283–294

Nagy D, Stacey AJ (1991) 3-D gravity modelling and discrete FFT performance on a pipelined vector supercomputer with interleaved memory. Proc Supercomputing Symp '91, Fredericton, pp 49–60

Nagy D, Baker DJ, Govindarajan R, Ross JW, VanKooten R, Yang H (1989) 3-dimensional gravity modelling: benchmarking the supercomputers. Proc Supercomputing Symp '89, University of Toronto, pp 125–134

Nagy D, Franke R, Battha L, Kalmár J, Papp G, Závoti J (1999) Comparison of various gridding methods. Acta Geod Geophys Hung 34: 41–57

Papp G (1996a) Modelling of the gravity field in the Pannonian Basin (in Hungarian). PhD thesis, Geodetic and Geophysical Research Institute Hungarian Academy of Sciences, Sopron

Papp G (1996b) On the application of physical filtering in 3-D forward gravity field modelling . In: Meurers B (ed) Proc 7th Int Meeting on Alpine Gravimetry. Österreichische Beiträge zu Meteorologie und Geophysik, Heft 14, pp 145–154 Zentralanstalt für Meteorologie und Geodynamik, Wien

Papp G, Benedek J (2000) Numerical determination of gravitational field lines – the effect of mass attraction on horizontal coordinates. J Geod 73: 648–659

Papp G, Kalmár J (1995) Investigation of sediment compaction in the Pannonian Basin using 3-D gravity modelling. Phys Earth Planet Int 88: 89–100

Papp G, Kalmár J (1996) Toward the physical interpretation of the geoid in the Pannonian Basin using 3-D model of the lithosphere. IGeS Bull 5: 63–87

Papp G, Wang ZT (1996) Truncation effects in using spherical harmonic expansions for forward local gravity field modelling. Acta Geod Geophys Hung 31: 47–66

Struik DJ (1988) Lectures on classical differential geometry, 2nd edn. Dover, New York

Tychonov AN, Samarski AA (1964) Differential equations of Mathematical Physics, vol 1. Holden-Day, San Francisco

Zach's Monatliche Correspondenz zur Beförderung der Erd- und Himmelskunde, (1811) November, Bd XXVII: 522